Whole-Exome Sequencing in Two Extreme Phenotypes of Response to VEGF-Targeted Therapies in Patients With Metastatic Clear Cell Renal Cell Carcinoma

Andre P. Fay, MD[a,*]; Guillermo de Velasco, MD[a,*]; Thai H. Ho, MD, PhD[b]; Eliezer M. Van Allen, MD[a,c]; Bradley Murray, BS[c]; Laurence Albiges, MD, PhD[a]; Sabina Signoretti, MD[d]; A. Ari Hakimi, MD[e]; Melissa L. Stanton, MD[f]; Joaquim Bellmunt, MD, PhD[a]; David F. McDermott, MD[g]; Michael B. Atkins, MD[g,h]; Levi A. Garraway, MD, PhD[a,c]; David J. Kwiatkowski, MD, PhD[i]; and Toni K. Choueiri, MD[a]

Abstract

Advances in next-generation sequencing have provided a unique opportunity to understand the biology of disease and mechanisms of sensitivity or resistance to specific agents. Renal cell carcinoma (RCC) is a heterogeneous disease and highly variable clinical responses have been observed with vascular endothelial growth factor (VEGF)–targeted therapy (VEGF-TT). We hypothesized that whole-exome sequencing analysis might identify genotypes associated with extreme response or resistance to VEGF-TT in metastatic (mRCC). Patients with mRCC who had received first-line sunitinib or pazopanib and were in 2 extreme phenotypes of response were identified. Extreme responders (ERs) were defined as those with partial response or complete response for 3 or more years (n=13) and primary refractory patients (PRPs) were defined as those with progressive disease within the first 3 months of therapy (n=14). International Metastatic RCC Database Consortium prognostic scores were not significantly different between the groups (*P*=.67). Considering the genes known to be mutated in RCC at significant frequency, *PBRM1* mutations were identified in 7 ERs (54%) versus 1 PRP (7%) (*P*=.01). In addition, mutations in *TP53* (n=4) were found only in PRPs (*P*=.09). Our data suggest that mutations in some genes in RCC may impact response to VEGF-TT.

J Natl Compr Canc Netw 2016;14(7):820–824

From the [a]Department of Medical Oncology, Dana-Farber Cancer Institute, Boston, Massachusetts; [b]Division of Hematology and Oncology, Mayo Clinic, Scottsdale, Arizona; [c]Broad Institute of MIT and Harvard, Cambridge, and [d]Department of Pathology, Brigham and Women's Hospital, Boston, Massachusetts; [e]Department of Surgery, Memorial Sloan Kettering Cancer Center, New York, New York; [f]Department of Laboratory Medicine/Pathology, Mayo Clinic, Scottsdale, Arizona; [g]Division of Hematology/Oncology, Beth Israel Deaconess Medical Center, Boston, Massachusetts; [h]Department of Medical Oncology, Georgetown-Lombardi Comprehensive Cancer Center, Washington, DC; and [i]Department of Medicine, Brigham and Women's Hospital, Boston, Massachusetts.

*These authors contributed equally to this manuscript.

Submitted October 23, 2015; accepted for publication March 21, 2016.

Dr. de Velasco has disclosed that his spouse receives salary from GlaxoSmithKline. Dr. Van Allen has disclosed that he receives consulting fees from or is a scientific advisor for Roche Ventana and Syapse. Dr. Albiges has disclosed that she is a scientific advisor for Novartis, Pfizer, Bayer, Sanofi, and Amgen, and receives research support from Novartis and Pfizer. Dr. Bellmunt has disclosed that he receives consulting fees from or is a scientific advisor for Astellas Pharma, Pfizer, and Pierre-Fabre; receives research support from Millennium and Sanofi; and has received compensation for travel, accommodations, expenses from MSD Oncology and Pfizer. Dr. McDermott has disclosed that he is on the data safety monitoring board for Pfizer; is a consultant for Bristol-Myers Squibb, Genentech BioOncology, Merck, Pfizer, Novartis, Eisai, Excelixis, and Array BioPharm; and receives research support from Prometheus. Dr. Atkins has disclosed that he receives consulting fees from or is a scientific advisor for Novartis, Pfizer, Genentech, Bristol-Myers Squibb, Merck, and GlaxoSmithKline. Dr. Garraway has disclosed that he receives consulting fees from and has equity interest in Foundation Medicine. Dr. Kwiatkowski has disclosed that he receives consulting fees from Novartis. Dr. Choueiri has disclosed that he receives institutional funding from Bristol-Myers Squibb, Exelixis, GlaxoSmithKline, Merck, Novartis, Pfizer, and TRACON Pharma, and is a scientific advisor for Bayer, GlaxoSmithKline, Merck, Novartis, and Pfizer. The remaining authors have disclosed that they have no financial interests, arrangements, affiliations, or commercial interests with the manufacturers of any products discussed in this article or their competitors.

This work was supported by the Trust family, Loker Pinard, and Michael Brigham Funds for Kidney Cancer Research (to Dr. Choueiri) at Dana-Farber Cancer Institute, the Dana-Farber/Harvard Cancer Center Kidney Cancer Program, the Dana-Farber/Harvard Cancer Center Kidney Cancer SPORE P50 CA101942-01, and by a grant from the Kidney Cancer Association. The authors declare that the research was conducted in the absence of any commercial or financial relationships that could be construed as a potential conflict of interest.

Correspondence: Toni K. Choueiri, MD, Lank Center of Genitourinary Oncology, Dana-Farber Cancer Institute/Brigham and Women's Hospital and Harvard Medical School, 450 Brookline Avenue, Boston, MA 02215. E-mail: Toni_Choueiri@dfci.harvard.edu

Recurrent molecular aberrations at the epigenetic, DNA, RNA, and protein levels have been identified in clear cell renal cell carcinoma (ccRCC).[1] Common emerging themes have evolved, including dysregulation of the von Hippel-Lindau (*VHL*) gene and chromatin remodeling pathways.[1] Kidney cancer genomics studies have identified recurrent mutations in novel tumor suppressors, such as chromatin-remodeling enzymes like *PBRM1* (33%–45% incidence),[2] *BAP1* (10%–15% incidence),[3] *JARID1C/KDM5C/SMCX* (3% incidence),[1] and *SETD2* (3%–12% incidence).[4] These mutations have been used to define molecular classifications associated with differences in tumor biology and prognosis,[5] but it is not known whether these tumor genotypes are associated with clinical response to treatment with vascular endothelial growth factor (VEGF)–targeted therapies (VEGF-TT), such as sunitinib or pazopanib. To examine a possible association between genomic alterations and response to VEGF-TT in RCC, we gathered patients with RCC with 2 distinct categories of response and performed whole-exome sequencing (WES) of pretreatment specimens.

Patients with metastatic RCC (mRCC) who received first-line sunitinib or pazopanib and were in 2 extreme phenotypes of response were identified. Extreme responders (ERs) were defined as those with partial or complete response (CR) for 3 or more years (n=13) and primary refractory patients (PRPs) were defined as those with progressive disease within the first 3 months of therapy (n=14). We performed WES in pretreatment formalin-fixed, paraffin-embedded samples (90% nephrectomies [n=18] and 10% lung metastases [n=2]) from 20 patients treated with sunitinib or pazopanib at Dana-Farber Cancer Institute. We also included 7 patients from The Cancer Genome Atlas (TCGA) treated with sunitinib or pazopanib in the metastatic setting who met the inclusion criteria. We used established Broad Institute analytical pipelines to identify point mutations and copy number alterations across the exome (see supplemental eAppendix 1, available with this article at JNCCN.org). In addition, a responder-enrichment algorithm was applied to identify genes selectively mutated in patients who were considered ERs.

The baseline characteristics of the ER cohort (n=13; PRP, n=14) are displayed in Table 1. No significant differences in International Metastatic RCC Database Consortium (IMDC) prognostic scores were identified between the 2 groups (*P*=.67). The top 5 recurrent mutations identified in the TCGA cohort, in which 22% of the samples were metastatic, were *VHL* (52%), *PBRM1* (33%), *SETD2* (12%), *BAP1* (10%), and *KDM5C* (7%).[1] In comparison, in our mRCC cohort, we detected *VHL*, *PBRM1*, *SETD2*, *BAP1*, and *KDM5C* mutations in 59%, 30%, 30%, 11%, and 11% of patients, respectively. We found the expected number of mutations for *PBRM1* and *KDM5C*. An increased rate of *BAP1* mutations has been associated with advanced clinical stage,[5] which might explain the elevated proportion in our series. The higher prevalence of *SETD2* mutations in our cohort is concordant with prior studies identifying *SETD2* loss of function in advanced RCC metastases.[6]

VHL was the most common gene mutated, with similar frequency in ERs (64%) and PRPs (50%) (Figure 1). Subsequently, *PBRM1*, *SETD2*, and *BAP1* were mutated in 30% (n=8), 30% (n=8), and 15% (n=4) of patients, respectively. *PBRM1* mutations were highly recurrently mutated in ERs (54% vs 7%; *P*=.01). Conversely, *TP53* mutations (n=4) were only identified in PRPs (*P*=.09). Interestingly, malfunction of p53 has been associated with resistance to sunitinib.[7] We did not identify other gene mutations associated with either response or primary refractory disease.

The WES approach was used to analyze outlier cases, and identified a potential association between somatic *PBRM1* mutations and favorable response to VEGF-TT in mRCC. Of interest is *PBRM1*, because it is the most commonly mutated chromatin-modifying gene in ccRCC. *PBRM1* contains bromodomains that interact with lysine-acetylated histones to regulate gene expression, and *PBRM1* mutations are associated with loss of PBRM1 expression.[3] Furthermore, a report from a phase III clinical trial has suggested that *PBRM1* might represent a predictive biomarker of benefit for targeted therapy.[8] Taken together, these results may lead to further modification of patient management.

Although our primary hypothesis was based on extreme patterns of response, we also found that *PBRM1* mutations and *TP53* mutations were associated with survival. Patients with *PBRM1* wild-type (WT) tumors had a median overall survival of 41.8 months versus not reached in the *PBRM1* mutant group (*P*=.04). Alternately, patients with *TP53* mu-

Table 1. Patient Characteristics

Variable	Extreme Responder (N=13) n (%)	Primary Refractory (N=14) n (%)	*P* Value[a]
Sex			–
Male	10 (76.9)	11 (78.6)	
Female	3 (23.1)	3 (21.4)	
Age, y (mean ± SD)	54.2 ± 8.8	54.6 ± 8.5	–
Nephrectomy			–
Yes	13 (100)	14 (100)	
No	0 (0)	0 (0)	
Prior cytokines			–
Yes	0 (0)	0 (0)	
No	13 (100)	14 (100)	
Time from diagnosis to treatment			.13
≤1 y	5 (38.5)	10 (71.4)	
>1 y	8 (61.5)	4 (28.6)	
Metastatic site			
Lung	9 (69.3)	9 (64.3)	
Bone	4 (28.6)	6 (42.9)	.69
Lymph node	3 (21.4)	5 (35.7)	.68
Liver	3 (21.4)	2 (14.3)	.65
Other	2 (14.3)	8 (57.1)	.046
Number of metastatic sites			.04
1	7 (53.8)	1 (7.7)	
2	4 (28.6)	7 (53.8)	
≥3	2 (14.3)	5 (38.4)	
Missing	0	1	
IMDC prognostic risk score			.67
Good	3 (23.1)	4 (30.8)	
Intermediate	10 (76.9)	8 (61.5)	
Poor	0 (0)	1 (7.7)	
Missing	0	1	
ECOG PS			–
0	11 (84.6)	12 (85.7)	
1	2 (15.4)	2 (17.3)	
VEGF-targeted therapy			.07
Sunitinib	7 (53.8)	9 (64.3)	
Pazopanib	6 (46.2)	2 (14.3)	
Sunitinib + gemcitabine	0 (0)	3 (21.4)	

Abbreviations: IMDC, International Metastatic Renal Cell Carcinoma Database Consortium; PS, performance score; VEGF, vascular endothelial growth factor.

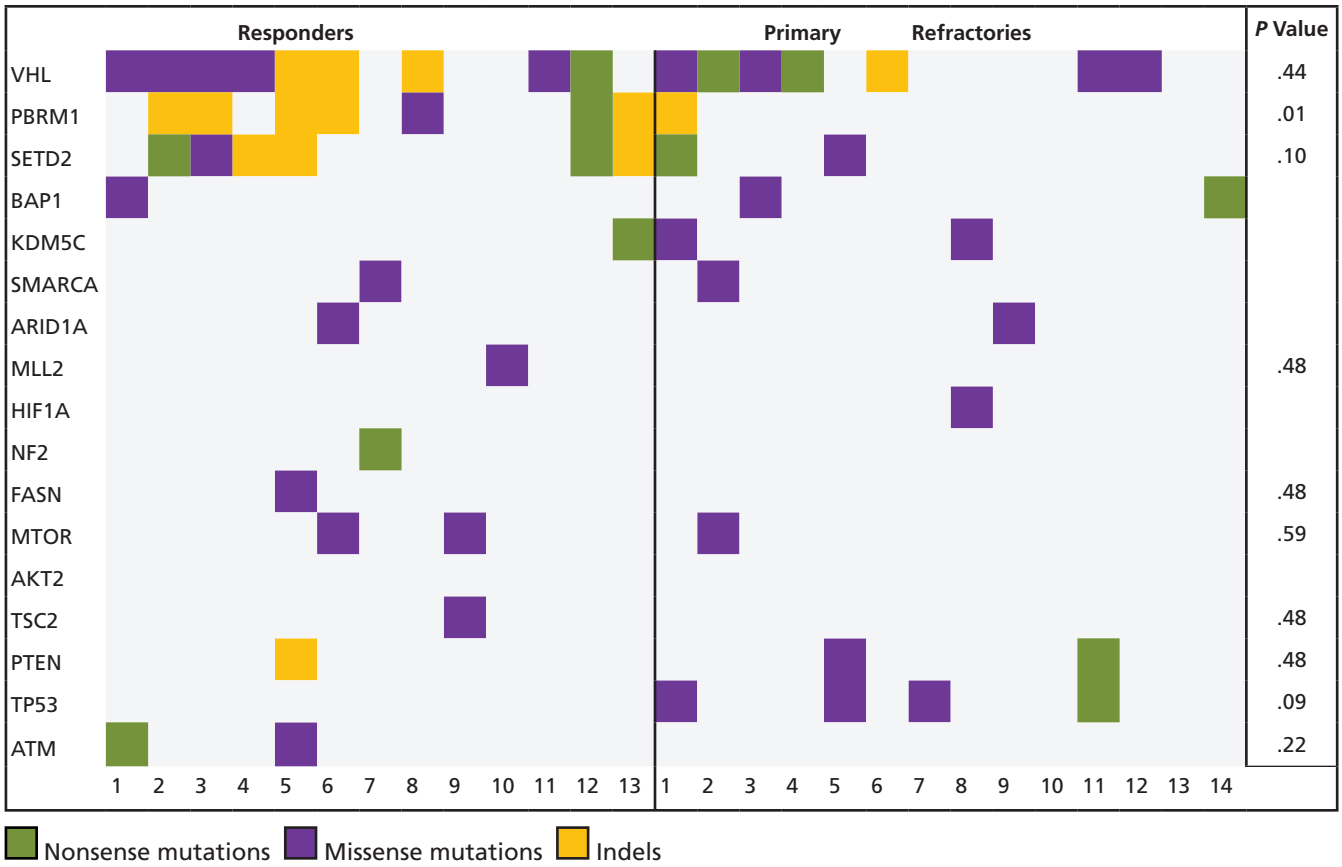

Figure 1. Representative map of mutations in respective genes according to response status.

tations achieved a median overall survival of 7.1 months versus not reached in patients with *TP53* WT tumors (*P*=.004). Despite our initial premise and selected population, these findings may suggest a prognostic role of such mutations, making it more difficult to distinguish between predictive and prognostic roles.

Our study has several limitations. First, it is important to mention that intratumor heterogeneity could be an important confounding factor. We only evaluated pretreatment specimens, and single specimens may not identify all subclone drivers during the evolution process. Moreover, the observed differences in mutation prevalence between TCGA and our cohort may reflect either the higher stage of presentation in our cohort or intratumor heterogeneity. It was estimated in a study of multiple biopsy cores from primary RCC tumors that a minimum of 3 distinct tumor regions are required for accurate tumor genotyping[9]; however, this is impractical in routine clinical care. These findings imply that larger studies with more statistical power are necessary to confirm our results. Second, although our mutation profiles were identified from metastatic tumors, we cannot determine whether these mutations are prognostic or predictive. As a prognostic algorithm, the IMDC has been externally validated and no significant differences in IMDC prognostic scores were identified between the 2 groups. There were also some baseline clinical differences between responders and nonresponders, such as the number of metastatic sites or the presence of "other" metastases. But there is not robust data suggesting such factors will determine sustained and durable responses. Although transcriptional profiling of *PBRM1*-mutant ccRCC tumors reveals a hypoxia signature, the molecular mechanism of how *PBRM1* mutations could alter clinical outcome of VEGF-TT is unclear.[2] Functional experiments are required to fully understand the mechanisms involved with these genomic alterations.

In conclusion, the discovery of mutations associated with divergent phenotypes of response aids in the understanding and development of molecular classifications of RCC. In a similar study of outliers,

mutations that converge on pathways of TSC1 inactivation and mTOR signaling hyperactivation have been associated with durable responses to rapalogs.[10] In our study, *PBRM1* mutations were associated with favorable responses to VEGF-TT in mRCC. The findings are suggestive only and hypothesis-generating; however, the potential of tumor genotypes to select treatment on the basis of genomic classifications is attractive and deserves further validation in a larger cohort.

References

1. Cancer Genome Atlas Research Network. Comprehensive molecular characterization of clear cell renal cell carcinoma. Nature 2013;499:43–49.
2. Varela I, Tarpey P, Raine K, et al. Exome sequencing identifies frequent mutation of the SWI/SNF complex gene PBRM1 in renal carcinoma. Nature 2011;469:539–542.
3. Peña-Llopis S, Vega-Rubín-de-Celis S, Liao A, et al. BAP1 loss defines a new class of renal cell carcinoma. Nat Genet 2012;44:751–759.
4. Dalgliesh GL, Furge K, Greenman C, et al. Systematic sequencing of renal carcinoma reveals inactivation of histone modifying genes. Nature 2010;463:360–363.
5. Gossage L, Murtaza M, Slatter AF, et al. Clinical and pathological impact of VHL, PBRM1, BAP1, SETD2, KDM6A, and JARID1c in clear cell renal cell carcinoma. Genes Chromosomes Cancer 2014;53:38–51.
6. Ho TH, Park IY, Zhao H, et al. High-resolution profiling of histone h3 lysine 36 trimethylation in metastatic renal cell carcinoma. Oncogene 2016;35:1565–1574.
7. Panka DJ, Liu Q, Geissler AK, Mier JW. Effects of HDM2 antagonism on sunitinib resistance, p53 activation, SDF-1 induction, and tumor infiltration by CD11b+/Gr-1+ myeloid derived suppressor cells. Mol Cancer 2013;12:17.
8. Hsieh J, Chen D, Wang P, et al. Identification of efficacy biomarkers in a large metastatic renal cell carcinoma (mRCC) cohort through next generation sequencing (NGS): results from RECORD-3 [abstract]. J Clin Oncol 2015;33(Suppl):Abstract 4509.
9. Sankin A, Hakimi AA, Mikkilineni N, et al. The impact of genetic heterogeneity on biomarker development in kidney cancer assessed by multiregional sampling. Cancer Med 2014;3:1485–1492.
10. Voss MH, Hakimi AA, Pham CG, et al. Tumor genetic analyses of patients with metastatic renal cell carcinoma and extended benefit from mTOR inhibitor therapy. Clin Cancer Res 2014;20:1955–1964.

See JNCCN.org for supplemental online content.

JNCCN
Journal of the National Comprehensive Cancer Network

Supplemental online content for:

Whole-Exome Sequencing in Two Extreme Phenotypes of Response to VEGF-Targeted Therapies in Patients With Metastatic Clear Cell Renal Cell Carcinoma

Andre P. Fay, MD; Guillermo de Velasco, MD; Thai H. Ho, MD, PhD; Eliezer M. Van Allen, MD; Bradley Murray, BS; Laurence Albiges, MD, PhD; Sabina Signoretti, MD; A. Ari Hakimi, MD; Melissa L. Stanton, MD; Joaquim Bellmunt, MD, PhD; David F. McDermott, MD; Michael B. Atkins, MD; Levi A. Garraway, MD, PhD; David J. Kwiatkowski, MD, PhD; and Toni K. Choueiri, MD

J Natl Compr Canc Netw 2016;14(7):820–824

- eAppendix 1: Supplemental Methods

eAppendix 1: Supplemental Methods

Patients and Samples

Formalin-fixed, paraffin-embedded (FFPE) samples from tumor and normal tissue from 20 patients with metastatic renal cell carcinoma (RCC) who met the inclusion criteria were retrieved. Slides were reviewed by an expert genitourinary pathologist (S.S.) and tumor cores were punched for DNA extraction. This project was approved by the Dana-Farber/Harvard Cancer Center (DF/HCC) Institutional Review Board (IRB) and the Peter MacCallum Cancer Center Ethics Committee or the Massachusetts Institute of Technology Committee on the Use of Humans as Experimental Subjects previous to clinical data collection and molecular analysis.

FFPE Sequencing

FFPE DNA Extraction

Paraffin is removed from FFPE sections and cores using CitriSolv (Fisher Scientific, Fair Lawn, NJ) followed by ethanol washes, then tissue is lysed overnight at 56°C. Samples are then incubated at 90°C to remove DNA crosslinks, and extraction is performed using QIAGEN's QIAamp DNA FFPE Tissue Kit (QIAGEN, Valencia, CA).

Library Construction

Initial genomic DNA input into shearing was reduced from 3 mcg to 10 to 100 ng in 50 mcL of solution. For adapter ligation, Illumina paired-end adapters were replaced with palindromic forked adapters, purchased from Integrated DNA Technologies, with unique 8-base molecular barcode sequences included in the adapter sequence to facilitate downstream pooling. With the exception of the palindromic forked adapters, the reagents used for end repair, A-base addition, adapter ligation, and library enrichment polymerase chain reaction (PCR) were purchased from Kapa Biosystems in 96-reaction kits. In addition, during the postenrichment solid-phase reversible immobilization (SPRI) bead cleanup, the elution volume was reduced to 20 mcL to maximize library concentration, and a vortexing step was added to maximize the amount of template eluted from the beads. Any libraries with concentrations less than 40 ng/mcL, as measured by a PicoGreen assay automated on an Agilent Bravo, were considered failures and reworked from the start of the protocol.

In-Solution Hybrid Selection

Also performed as previously described with the following modifications to the hybridization reaction: before hybridization, any libraries with concentrations greater than 60 ng/mcL as determined by PicoGreen were normalized to 60 ng/mcL, and 8.3 mcL of library was combined with blocking agent, bait, and hybridization buffer. Any libraries with concentrations between 50 and 60 ng/mcL were normalized to 50 ng/mcL, and 10.3 mcL of library was combined with blocking agent, bait, and hybridization buffer. Any libraries with concentrations between 40 and 50 ng/mcL were normalized to 40 ng/mcL, and 12.3 mcL of library was combined with blocking agent, bait, and hybridization buffer. Regardless of library concentration range, the same volume of blocking agent and bait previously described were used, and hybridization buffer volume was adjusted to equal the combined volume of library, blocking agent, and bait. Finally, the hybridization reaction was reduced to 17 hours with no changes to the downstream capture protocol.

Preparation of Libraries for Cluster Amplification and Sequencing: After postcapture enrichment, libraries were quantified using PicoGreen (automated assay on the Agilent Bravo), normalized to equal concentration on the Perkin-Elmer MiniJanus, and pooled by equal volume on the Agilent Bravo Automated Liquid Handling Platform. Library pools were then quantified using quantitative PCR (kit purchased from Kapa Biosystems) with probes specific to the ends of the adapters; this assay was automated using Agilent's Bravo Automated Liquid Handling Platform. Based on quantitative PCR (qPCR) quantification, libraries were normalized to 2 nM, and then denatured using 0.2 N of NaOH on the Perkin-Elmer MiniJanus. After denaturation, libraries were diluted to 20 pM using hybridization buffer purchased from Illumina.

eAppendix 1: Supplemental Methods (cont.)

Cluster Amplification and Sequencing: Cluster amplification of denatured templates was performed according to the manufacturer's protocol (Illumina) HiSeq v3 cluster chemistry and flowcells, as well as Illumina's Multiplexing Sequencing Primer Kit. Flowcells were sequenced using HiSeq 2000 v3 Sequencing-by-Synthesis Kits, then analyzed using RTA v.1.12.4.2 or later. Each pool of whole-exome libraries was run on paired 76-bp runs, and 8-base index sequencing read was performed to read molecular indices, across the number of lanes needed to meet coverage for all libraries in the pool.

Analysis and Interpretation

DNA Assembly and Quality Control

Sequence Data Processing: Exomes sequence data processing was performed using established pipelines at the Broad Institute. A BAM file was produced with the Picard pipeline (http://picard.sourceforge.net/), which aligns the tumor and normal sequences to the hg19 human genome build using Illumina sequencing reads. The BAM was uploaded into the Firehose pipeline (http://www.broadinstitute.org/cancer/cga/Firehose), which manages input and output files to be executed by GenePattern. Whole-exome sequencing BAM files for data from this study cases will be deposited in dbGAP (phs001018).

Sequencing Quality Control: Quality control modules within Firehose were applied to all sequencing data for comparison of the origin for tumor and normal genotypes and confirm fingerprinting concordance. Cross-contamination of samples was estimated using ContEst41 to confirm that neither tumor nor germline sample had more than 3% contamination. Single-nucleotide polymorphism fingerprints from each lane of a tumor/normal pair were crosschecked to confirm concordance, and nonmatching lanes were removed from analysis. Somatic alteration identification and annotation The MuTect algorithm was applied to identify somatic single-nucleotide variants in targeted exons. Indelocator (http://www.broadinstitute.org/cancer/cga/indelocator) was applied to identify small insertions or deletions. Annotation of identified variants was performed using Oncotator (http://www.broadinstitute.org/cancer/cga/oncotator). Rearrangements were identified using dRanger (http://www.broadinstitute.org/cancer/cga/dranger). Copy ratios were calculated for each hybrid capture bait by dividing the tumor coverage by the median coverage obtained in a set of reference normal samples. The resulting copy ratios were segmented using the circular binary segmentation algorithm. Genes in copy ratio regions with segment means of greater than log2(4) were evaluated for focal amplifications given the potential clinical significance of a large focal event. Genes in regions with segment means of less than log2(0.5) were evaluated for hemizygous or homozygous deletions, because either broad or focal deletions may involve genes with clinical relevance. RefSeq was used to identify the genes that reside in the chromosomal coordinates demarcated by the segment start and end points.